Proceedings of the 4th Jagiellonian Symposium on Advances in Particle Physics and Medicine

Helicity Dependent Cross-Sections for the Photoproduction of $\pi^0\pi^{+/-}$ Pairs from Quasi-Free Nucleon Targets

D. Ghosal* for the A2 Collaboration

Department of Physics, University of Basel, Ch-4056 Basel, Switzerland

Doi: 10.12693/APhysPolA.142.347
*e-mail: debdeep.ghosal@unibas.ch

Using the MAMI-C microtron at an accelerator facility in Mainz, Germany, fixed target experiments carry on to study the excitation spectrum of the nucleon via the photoproduction of mesons. In this paper, the photon-induced production of the $\pi^0\pi^\pm$-pairs with a liquid deuterium target has been investigated in view of the helicity dependence of the two isospin channels. While unpolarized cross-sections for protons and neutrons have been extracted, this data alone is not sufficient to separate the resonances, therefore polarization observables are vital factors essential in disentangling the contributing resonant and non-resonant amplitudes. The double-polarization observable E was extracted with the help of a longitudinally polarized deuterated butanol target and a circularly polarized photon beam. The antiparallel and parallel spin configurations between the beam photon and the target nucleon imply the spin-dependent cross-sections $\sigma_{1/2}$ and $\sigma_{3/2}$, respectively, which have been derived from E. Reaction products were detected with an almost 4π solid-angle covering calorimeter composed of the Crystal Ball, TAPS detectors, and particle identification detectors. The results are sensitive to sequential decays of nucleon resonances that include intermediate states and also involve the emission of charged ρ mesons. Furthermore, comparative studies of the results of the most recent available model calculations were made.

topics: meson photoproduction, pion pairs, helicity asymmetry

1. Introduction

With the help of quark models, the behavior of quarks in nucleons can be described at medium energies. Meson photoproduction [1] is an effective tool to study excited states (resonances) of nucleons. Unfortunately, many states with larger widths and shorter lifetime overlap with each other and cannot be easily disentangled; so far, many of them have been predicted but not yet detected [2]. Those unobserved states may be missing because of some experimental bias, or they may not exist at all. Most earlier experiments were performed with pion beams, as a result of which some resonances might couple weakly to pions and more strongly to rare channels, thus avoiding detection. To date, most results arise from experiments on the proton [3], which do not provide much information regarding the isospin structure of electromagnetic transitions. Therefore, advances in neutron experiments may consolidate the understanding of the nucleon spectrum [4]. Unfortunately, free neutron target does no exist, although a deuterated butanol target has made it possible to study spin effects with quasi-free neutrons.

From the outcomes of an older total absorption experiment [5, 6], possible significant contribution from the $D_{13}(1520) \to N\rho$ decay became a hot topic, because this could also modify the shape of D_{13} [6] due to the predicted in-medium modifications [7] of the ρ meson. One further motivation for present experiments with proton and deuteron targets is that the $D_{13} \to N\rho$ branching ratio for proton and neutron targets was extracted much more precisely.

For years, cross-section data has been used to study the nucleon spectrum, however this data alone is not sufficient to distinguish broad overlapping resonances (the "missing resonance" issue). Instead, model-independent polarization observables can support understanding of these overlapping resonances by focusing on hidden information about the complex helicity amplitudes [8]. Here, the observable E will be discussed. It will be analyzed in two versions determined by polarization. The cross-section and the polarization observable E can be related in terms of the helicity of the beam and the target as follows [9]

$$E_{\mathrm{version1}} = \frac{\sigma_{1/2} - \sigma_{3/2}}{\sigma_{1/2} + \sigma_{3/2}} = \frac{\sigma_{\mathrm{diff}}}{\sigma_{\mathrm{sum}}}, \tag{1}$$

$$E_{\mathrm{version2}} = \frac{\sigma_{\mathrm{diff}}}{2\sigma_{\mathrm{unpol.}}}, \tag{2}$$

where $\sigma_{1/2}$ is the cross-section for the case where the beam and target polarizations are anti-parallel; $\sigma_{3/2}$ is the cross-section when they are parallel.

2. Experimental setup

The measurements have been conducted at the MAMI-C accelerator facility in Mainz, Germany [10]. A longitudinally polarized electron beam with energy $\sim$ 1.5 GeV and polarization degree 80% [11] is used for the A2 experiment. Circularly polarized photons are generated by a copper radiator and their energy is tagged using the Glasgow-Mainz photon tagger [3, 12]. The target is made of deuterated butanol material (dButanol) and is transversally or longitudinally polarized up to 80%. The target is surrounded by a cylindrically shaped particle identification detector (PID) [13] consisting of 24 plastic scintillator strips, each covering 15° in the azimuthal angle. Around PID, there is a multi-wire proportional chamber (MWPC) which is further surrounded by the spherical shaped Crystal Ball (CB) calorimeter [14]. This CB is made up of 672 NaI(Tl) crystals and it covers 20°–160° in the polar angle. In the forward direction, the Two Arms Photon Spectrometer (TAPS) calorimeter [15] is present which consists of 72 $PbWO_4$ crystals (the two innermost rings) and 366 BaF_2 crystals (remaining rings). A veto wall in front of TAPS is installed for further particle identification. Together, CB and TAPS provide an acceptance of almost 4π in the center of mass frame and ensure high angular and energy resolution.

3. Analysis: extraction of asymmetries and helicity-dependent cross-sections

With the help of information registered in the detectors, events are accumulated, and then selected based on the number of charged or neutral hits. Neutral mesons are identified by the χ^2 test, with the best combination of photon clusters for the meson invariant mass. In order to eliminate accidentally coincident tagger photons, coincidence time cuts are applied and random background subtraction is performed. Furthermore, kinematic cuts are applied for each W (center of mass energy) and and each angular interval of the pion–pion system in the beam direction, so that background can be isolated from the signal.

The analysis of $\gamma p(n) \to \pi^0\pi^+ n(n)$ demands the detection of the decay photons of the π^0 meson along with the π^+ meson and the recoil neutron. Therefore, all events with 3 neutral clusters and 1 charged cluster are selected. The $(E - \Delta E)$ analysis was used to identify the charged pion by comparing the energy deposition in CB and the energy loss in PID [16].

In the case of $\gamma n(p) \to \pi^0\pi^- p(p)$, the decay photons of the mesons π^0 and π^-, as well as the recoil proton, must be identified. Hence, all events with 2 neutral clusters and 2 charged clusters are needed to be selected. For both reactions, the nucleon in brackets was the undetected spectator nucleon.

In addition, the pulse-shape analysis shows that in response of the BaF_2 crystal to the pulse, the separation of photons and neutrons occurs [9]. Time-of-flight versus energy analysis provides additional separation of protons, photons, and neutrons.

Now, further step of event identification start with the invariant mass analysis of the two decay photons of the π^0 meson [17]. The next step of event identification involved suppressing the background from other reactions that have a neutral, charged pion and a recoil nucleon in the final state, but also additional particles that went undetected. Critical are triple-pion production processes (including the reaction $\gamma N \to N\eta \to N\pi^0\pi^+\pi^-$), where one charged pion can be lost or misidentified as a recoil proton [9].

Although the "coplanarity" condition (i.e., the azimuthal angles of the momenta of the recoil nucleon and the two-pion system must be back-to-back in the laboratory frame) can be simply satisfied at this point, nevertheless this condition is not fully reliable because undetected charged pions with low momenta do not heavily influence the angular balance. Rather, missing mass analysis may be more suited where the recoil nucleon, although detected, is treated as the missing particle and its mass is calculated from the kinematic parameters of the meson pair [9].

The asymmetry of E is defined by (2) in Sect. 1. In principle, it follows directly from the count rates of the reaction for the two helicity states ($\uparrow\uparrow$) ($N_{3/2}$) and ($\uparrow\downarrow$) ($N_{1/2}$) by

$$E = \frac{1}{P_\odot P_T}\,\frac{N_{1/2}-N_{3/2}}{\left(N_{1/2}-N_B\right)+\left(N_{3/2}-N_B\right)}, \qquad (3)$$

where $P_\odot$ and P_T are the beam and target polarization degrees, respectively, and N_B is the background count rate for unpolarized nucleons bound in heavy nuclei of the butanol molecules that cancels in the numerator. Due to this, background count rate measurements with carbon and/or liquid deuteron targets are also needed.

Two approaches were used for the extraction of the beam asymmetry E, details of which can be found in [3].

One can determine the final-state W from four vectors of the final state particle [18], which are actually measured with lower experimental resolution than the energy of the incident photon. The problem outlined here is more difficult at higher energies, because the kinetic energies of the charged pions are far less determined than the photon energies, due to the punch-through of the particles.

4. Results and discussion

The results for the total asymmetry E integrated over all meson angles and invariant mass distributions are shown in Fig. 1 for both the reaction amplitudes as a function of the incident photon energy E_γ and the final state energy W.

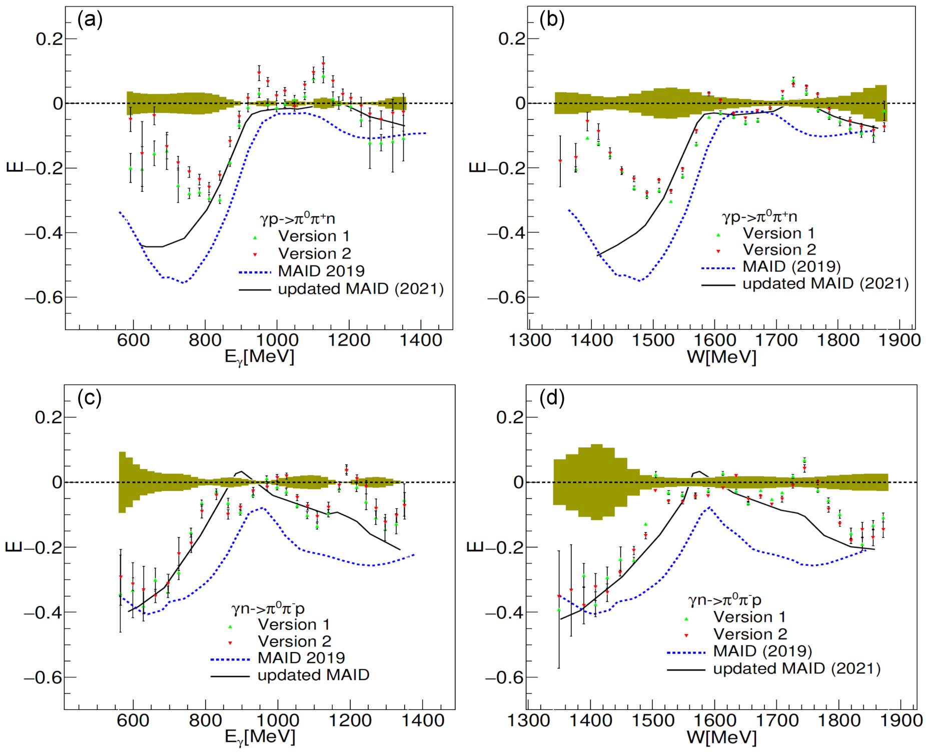

Fig. 1. Plots of E observable as a function of E_γ (photon energy) and W(center of mass energy) for $\gamma p \to \pi^0\pi^+ n$ (respectively, panels (a) and (b)) and for $\gamma n \to \pi^0\pi^- p$ (respectively, (c) and (d)). The red triangles are for the method with carbon subtraction and the green ones correspond to the direct method. The blue dotted line corresponds to the older MAID model (before the inclusion of the present data), while the solid black lines correspond to the updated MAID model [19].

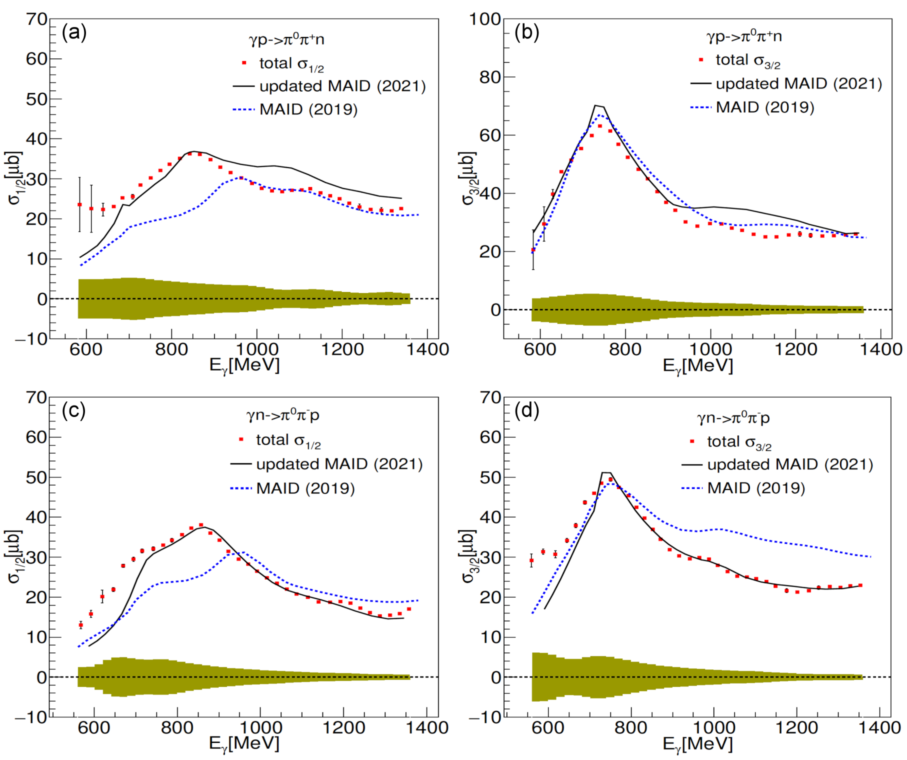

Fig. 2. Total cross-section comparison for $\gamma p(n) \to \pi^0\pi^+ n(n)$ ((a) and (b) panels) and $\gamma n(p) \to \pi^0\pi^- p(p)$ ((c) and (d)). The red squared symbols in each panel represent data points, the blue dotted line shape corresponds to the older MAID model, while the solid black lines correspond to the updated MAID model.

Figure 1 summarizes the results from the two analyses and the predicted MAID model, which agree very well, demonstrating that the elimination of unpolarized background is well controlled. For the further analysis of the $\sigma_{1/2}$ and $\sigma_{3/2}$ components of the cross-section, the average of the two results for E were used. The statistical uncertainties of E were linearly averaged because they are dominated by the fluctuations of the numerator in (2), which is identical for both analyses. Figure 2 shows the total cross-sections for proton and neutron targets as functions of E_γ and W. They are compared to the fits with the MAID model [19]. Inclusion of the present data in the fits has improved the agreement between the data and the model fit (updated MAID) as expected.

5. Conclusions

The original motivation for this analysis was a better basis for the simulation of detection efficiencies, which can be quite different for reactions with different intermediate states depending on the kinematics ($\Delta^0\pi^+$, $\Delta^+\pi^0$ and ρ^+n for the γp initial state and $\Delta^0\pi^0$, $\Delta^+\pi^-$ and ρ^-p for the γn initial state). However, the result gives also the first hints at the involved physics of the reaction.

In summary, precise data have been obtained for the helicity dependence of photoproduction of mixed-charge pion pairs of nucleons and compared with the available model predictions. A more refined combined analysis of several new data sets for the photoproduction of pion pairs is still in process.

Acknowledgments

All of the results presented here have been obtained inside A2 collaboration at the Mainz MAMI accelerator. The support from Swiss National Fund (SNF) is kindly acknowledged.

References

[1] S.D. Bass, P. Moskal, *Rev. Mod. Phys.* **91** (2019).

[2] R.G. Edwards, J.J. Dudek, D.G. Richards, S.J. Wallace, *Phys. Rev. D* **84**, 074508 (2011).

[3] D. Ghosal, *Acta Phys. Pol. B* **51**, 245 (2020).

[4] B. Krusche, Photoproduction of Mesons off Nuclei and In-Medium Modifications of Hadrons, DNP Annual Meeting, Oakland 2008.

[5] N. Bianchi, V. Muccifora, E. De Sanctis et al., *Phys. Lett. B* **325** (1993).

[6] F. Zehr, B. Krusche, P. Aguar et al., *Eur. Phys. J. A* **48**, 98 (2012).

[7] B. Krusche, J. Ahrens, R. Beck, I.J.D. MacGregor, J.C. McGeorge, V. Metag, H. Ströher, *Phys. Rev. Lett.* **86**, 4764 (2001).

[8] D. Ghosal, *Eur. Phys. J. Web Conf.* **241** (2020).

[9] D. Ghosal, Ph.D. Thesis, University of Basel, 2021.

[10] K.H. Kaiser, K. Aulenbacher O. Chubarov et al., *Nucl. Instrum. Methods Phys. Res. A* **593**, 159 (2008).

[11] N.K. Walford, *AIP Conf. Proc.* **1735**, 040012 (2016).

[12] J.C. McGeorge, J.D. Kellie, J.R.M. Annand et al., *Eur. Phys. J. A* **37**, 129 (2008).

[13] D. Watts, in: *Calorimetry in Particle Physics, Proceedings of the 11th Int. Conf., Perugia (Italy) 2004*, Eds. C. Cecchi, P. Cenci, P. Lubrano, M. Pepe, World Scientific, Singapore 2005, p. 560.

[14] A. Starostin, B.M.K. Nefkens, E. Berger et al. (The Crystal Ball Collaboration), *Phys. Rev. C* **64**, 55205 (2001).

[15] A.R. Gabler, W. Döring, M. Fuchs et al., *Nucl. Instrum. Methods Phys. Res. A* **346**, 168 (1994).

[16] A. Kaeser, Ph.D. Thesis, University of Basel, 2017.

[17] M. Oberle, Ph.D. Thesis, University of Basel, 2014.

[18] D. Werthmüller, L. Witthauer, I. Keshelashvili et al. (A2 Collaboration at MAMI), *Phys. Rev. C* **90**, 015205 (2014).

[19] A. Fix, H. Arenhovel, *Phys. Rev. C* **83**, 015503 (2011).